Electronic Supplementary Information

Tuning copper(II) ion selectivity: The role of basicity, size of chelating ring and orientation of coordinating atoms

Narendra Reddy Chereddy [a], Purna Sai Korrapati[b], Sathiah Thennarasu*[a] and Asit Baran Mandal*[b]

[a]*Organic Chemistry Division,* [b]*Biomaterials Laboratory,* [c]*Chemical Laboratory, CSIR-Central Leather Research Institute, Adyar, Chennai-600 020, India*

Corresponding author Tel.: +91 44 24913289; Fax: +91 44 24911589
E-Mail: thennarasu@gmail.com, abmandal@hotmail.com

Table of contents **Page**

Experimental section, synthesis and characterisation of the probes S2-S5

^{1}H- and ^{13}C-NMR spectra of **1, 2** and **3** (Figures S1-S6) S6-S11

ESI-MS analytical data of **1, 2** and **3** (Figures S7-S9) S12-S14

ESI-MS analytical data of **1**-Cu^{2+}, **2**-Cu^{2+}, and **3**-Cu^{2+} complexes (Figures S10-S12) S15-S17

The Job plot data of **1-Cu^{2+}** (**a**) and **3-Cu^{2+}** (**b**) complexes (Figure S13) S18

^{13}C-NMR spectra of **3** in the presence of various amounts of Cu^{2+} (Figure S14) S19

FT-IR spectra of **3** and **3**-Cu^{2+} complex (Figure S15) S20

ESR spectrum of **3**-Cu^{2+} complex (Figure S16) S21

Variation in the absorption intensity of **1** and **3** with Cu^{2+} (Figure S17) S22

Gaussian 03; b3lyp/6-31(d) optimized conformation of **1** (Figure S18) S23

Gaussian 03; b3lyp/6-31(d) optimized conformation of **3** (Figure S19) S24

Gaussian 03; b3lyp/LANL2DZ optimized geometry of **3-Cu^{2+}** complex (Figure S20) S25

Metal ion competitive experiments of **3** (Figure S21) S26

EDTA experiments to confirm the reversibility of **3-Cu^{2+}** complex (Figure S22) S27

pH dependent variation in fluorescence intensity of **3** (Figure S23) S28

NIH3T3 Cell viability assay (Figure S24) S29

Energies of different conformers of **1** (Figure S25) S30

Energies of different conformers of **3** and **3-Cu^{2+}** complex (Figure S26) S31

Experimental Section

Dry acetonitrile and double distilled water were used in all experiments. All the materials for synthesis were purchased from commercial suppliers and used without further purification. The solutions of metal ions were prepared from the corresponding chloride salts. Absorption spectra were recorded on a SPECORD 200 PLUS UV-Visible spectrophotometer. Fluorescence measurements were performed on a HITACHI F-4500 fluorescence spectrophotometer (Excitation wavelength 520 nm; Slit width 5 nm). The fluorescence and absorption measurements were carried out using 0.01 M Tris HCl-CH_3CN (1:1 v/v mixture, pH 7.4) as the solvent. The quantum yield of free rhodamine B in 0.01 M Tris HCl-CH_3CN (1:1 v/v mixture, pH 7.4) was assumed to be 1.00, and the quantum yields of **3** and **3-Cu^{2+}** complex were determined as reported in the literature.[1] This information is included in the revised supporting information.All pH measurements were made with a Systronics μpH System Model 361. NMR spectra were recorded using a JEOL–ECP500 spectrometer operating at 500 MHz. ESI-MS spectra were obtained on a Thermo Finnigan LCQ Advantage MAX 6000 ESI mass spectrometer. Fluorescence imaging experiments were performed using a Leica DM IRB microscope equipped with EBQ-100 UV-lamp. Green channel (Emission filter LP 515) was used as the excitation source and the fluorescence response was measured using the red channel (Emission filter LP 590). DFT calculations were performed using Gaussian 03 at the b3lyp/6-31(d) level. All measurements were carried out at room temperature. Stock solutions of rhodamine derivatives (probes) were prepared by dissolving 1.0 mmol of probes (6.75 mg, 6.74 mg and 7.55 mg of **1**, **2** and **3**, respectively) in 1:1 v/v 0.01M Tris HCl-CH_3CN (pH 7·4) separately, and making up to the mark in a 10 mL volumetric flask. Further dilutions were made to prepare 100 μM solutions for the

experiments. Stock solutions of all amino acids (1 M) and metal ions (1 M) were prepared in de-ionised water.

Synthesis of rhodamine 6G hydrazide A

Rhodamine B hydrazide was synthesized according to the reported procedure.[2]

Synthesis of picolyl or benzyl appended indole-3-corboxaldehyde B or C

The picolyl or benzyl appended indole-3-corboxaaldehyde **B** or **C** was synthesized in a single step procedure. To a solution of indole-3-carboxaldehyde (0.72 g, 5 mmol) and potassium carbonate (1.04 g, 7.5 mmol) in DMF (20 mL) was added 2-(Chloromethyl)pyridine hydrochloride (0.99 g, 6.0 mmol) or benzyl bromide (1.02 g, 6.0 mmol) and the solution was stirred at room temperature overnight. After completion of reaction monitored using TLC, the reaction mixture was partitioned between DCM and water, the DCM layer was collected. The aqueous layer was extracted three times with DCM, the combined organic extracts was dried over anhydrous Na_2SO_4, concentrated under vacuum and then subjected to silica gel column chromatography to obtain the desired product.

Synthesis of triazole appended indole-3-corboxaldehyde D

The triazole appended indole-3-corboxaaldehyde **D** was synthesized in a two-step procedure. To a solution of indole-3-carboxaldehyde (0.72 g, 5 mmol) and potassium carbonate (1.04 g, 7.5 mmol) in DMF (20 mL), propargyl bromide (0.7 mL, 7.5 mmol) was added drop wise and the resulting mixture was allowed to stir overnight at room temperature. After completion of reaction monitored using TLC, the reaction mixture was partitioned between DCM and water, the DCM layer was collected. The aqueous layer was extracted three times with DCM, the combined organic extracts was dried over anhydrous Na_2SO_4 and concentrated under vacuum to obtain the desired propargylated aldehyde that was later on converted to a triazole

derivative using click chemistry. Propargylated aldehyde (0.55 g, 3 mmol) was dissolved in 1:1 THF/H_2O mixture and triethyl amine (0.7 mL, 5 mmol) was added. Sodium azide (0.26 g, 4 mmol), benzyl bromide (0.48 mL, 4 mmol) and cuprous iodide (c.a) were added to this solution. The resulting mixture was allowed to stir overnight at room temperature. Upon completion of the reaction monitored by TLC, the mixture was filtered, extracted with ethyl acetate, concentrated under vacuum and then subjected to silica gel column chromatography to obtain the desired product.

Synthesis of rhodamine probes 1 and 2

To a solution of rhodamine B hydrazide **A** (0.46 g, 1 mmol) dissolved in 20 mL methanol, picolyl or benzyl appended indole-3-corboxaaldehyde **B** or **C** (0.26 g, 1.1 mmol) was added. The mixture thus obtained was refluxed in an oil bath for ~3h. After that, the solution was cooled to room temperature. The white precipitate formed upon cooling was filtered and dried in vacuum to obtain 0.52 g of **1** (79% yield) and 0.53 g of **2** (80% yield).

The NMR and ESI-MS data of the probe **1**. ^{1}H NMR ($CDCl_3$, 500 MHz), δ (ppm): 1.12 (t, J = 7.0 Hz, 12H, $NCH_2\underline{CH_3}$), 3.29 (q, , J = 7.0 Hz, 8H, $N\underline{CH_2}CH_3$), 5.31 (s, 2H, CH_2), 6.24 (dd, J = 2.5 Hz, 2H, Xanthene-H), 6.47 (d, J = 2.5 Hz, 2H, Xanthene-H), 6.55 (dd, J = 3.0 Hz, 2H, Xanthene-H), 6.65 (d, J = 7.5 Hz, 1H, Ar-H), 7.07-7.20 (m, 5H, Ar-H), 7.32 (s, 1H, Ar-H), 7.41-7.51 (m, 3H, Ar-H), 7.95-8.01 (m, 2H, Ar-H), 8.52 (d, J = 4.5 Hz, 1H, Ar-H), 9.37 (s, 1H, Imine-H). ^{13}C NMR ($CDCl_3$, 125 MHz), δ (ppm): 12.74, 44.42, 52.25, 66.59, 97.97, 106.98, 107.93, 109.49, 114.00, 120.93, 121.19, 122.71, 123.08, 123.61, 124.09, 125.87, 128.34, 128.51, 131.29, 131.91, 132.79, 137.09, 137.21, 146.45, 148.79, 149.54, 151.11, 153.77, 156.79, 164.20; ESI-HRMS (+ve mode, m/z): 675.3443 ($M+H^+$), Calc. for $C_{43}H_{43}N_6O_2$ is 675.3447.

The NMR and ESI-MS data of the probe **2**. ^{1}H NMR ($CDCl_3$, 500 MHz), δ (ppm): 1.13 (t, *J* = 7.0 Hz, 12H, $NCH_2\underline{CH_3}$), 3.29 (q, , *J* = 7.0 Hz, 8H, $N\underline{CH_2}CH_3$), 5.19 (s, 2H, CH_2), 6.24 (dd, *J* = 2.5 Hz, 2H, Xanthene-H), 6.46 (d, *J* = 2.0 Hz, 2H, Xanthene-H), 6.54 (d, *J* = 8.0 Hz, 2H, Xanthene-H), 7.03-7.11 (m, 3H, Ar-H), 7.12-7.19 (m, 3H, Ar-H), 7.22-7.29 (m, 4H, Ar-H), 7.46-7.50 (m, 2H, Ar-H), 7.96 (d, *J* = 6.0 Hz, 2H, Ar-H), 9.35 (s, 1H, Imine-H). ^{13}C NMR ($CDCl_3$, 125 MHz), δ (ppm): 12.74, 44.42, 52.35, 66.59, 97.97, 106.96, 107.93, 109.52, 113.56, 121.05, 122.92, 123.06, 123.45, 124.07, 125.85, 126.95, 127.89, 128.32, 128.48, 128.90, 131.28, 131.71, 132.76, 136.71, 137.19, 146.51, 148.79, 151.12, 153.75, 164.18; ESI-HRMS (+ve mode, m/z): 674.3497 ($M+H^+$), Calc. for $C_{44}H_{44}N_5O_2$ is 674.3495.

Synthesis of rhodamine probe 3

To a solution of rhodamine 6G hydrazide **A** (0.46 g, 1 mmol) dissolved in 20 mL methanol, triazole appended indole-3-corboxaldehyde **D** (0.34 g, 1.1 mmol) was added. The red colour mixture thus obtained was refluxed in an oil bath for ~3h and the solution was cooled to room temperature. The white precipitate formed was filtered and dried in vacuum to obtain 0.50 g of **3** (70% yield).

^{1}H NMR ($CDCl_3$, 500 MHz), δ (ppm): 1.07 (t, *J* = 6.5 Hz, 12H, $NCH_2\underline{CH_3}$), 3.22 (q, , *J* = 7.0 Hz, 8H, $N\underline{CH_2}CH_3$), 5.07 (s, 2H, CH_2), 5.15 (s, 2H, CH_2), 6.17 (dd, *J* = 3.0 Hz, 2H, Xanthene-H), 6.44 (d, *J* = 7.5 Hz, 2H, Xanthene-H), 6.49 (s, 1H, Xanthene-H), 6.51 (s, 1H, Xanthene-H), 6.94 (s, 1H, Xanthene-H), 6.98 (s, 1H, Xanthene-H), 7.01-7.04 (m, 2H, Ar-H), 7.05-7.11 (m, 2H, Ar-H), 7.13-7.18 (m, 2H, Ar-H), 7.18-7.23 (m, 3H, Ar-H), 7.45-7.49 (m, 2H, Ar-H), 7.95-7.97 (m, 2H, Ar-H), 9.22 (s, 1H, Imine-H). ^{13}C NMR ($CDCl_3$, 125 MHz), δ (ppm): 12.71, 44.38, 49.50, 53.97, 66.56, 97.91, 106.85, 107.90, 109.61, 113.45, 121.22, 122.14, 123.07, 123.39, 124.06, 125.67, 128.05, 128.39, 128.65, 129.03, 131.14, 131.38, 132.85,

134.58, 136.68, 144.11, 146.50, 148.76, 151.07, 153.72, 164.16; ESI-HRMS (+ve mode, m/z): 755.3823 ($M+H^+$), Calc. for $C_{47}H_{47}N_8O_2$ is 755.3822.

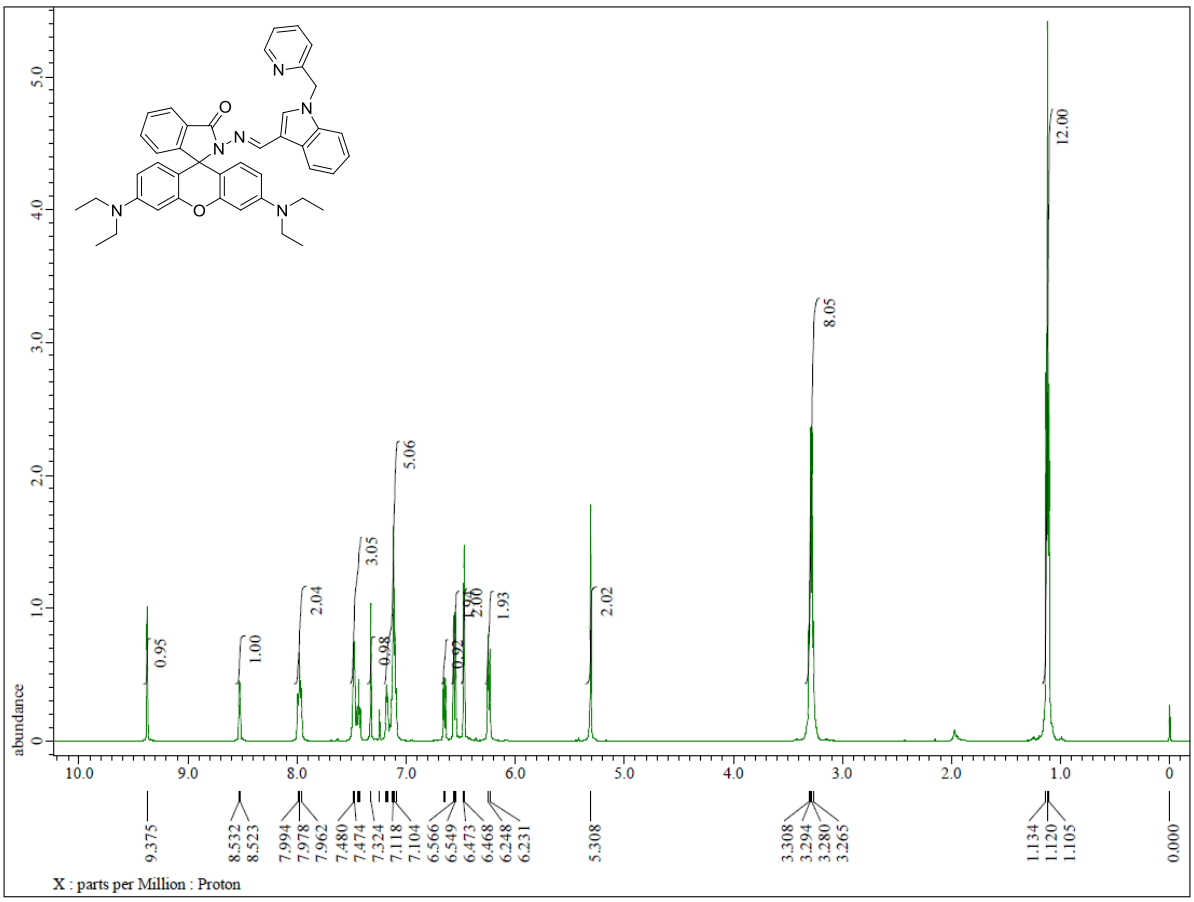

Fig. S1. ^{1}H NMR spectrum of **1** in $CDCl_3$

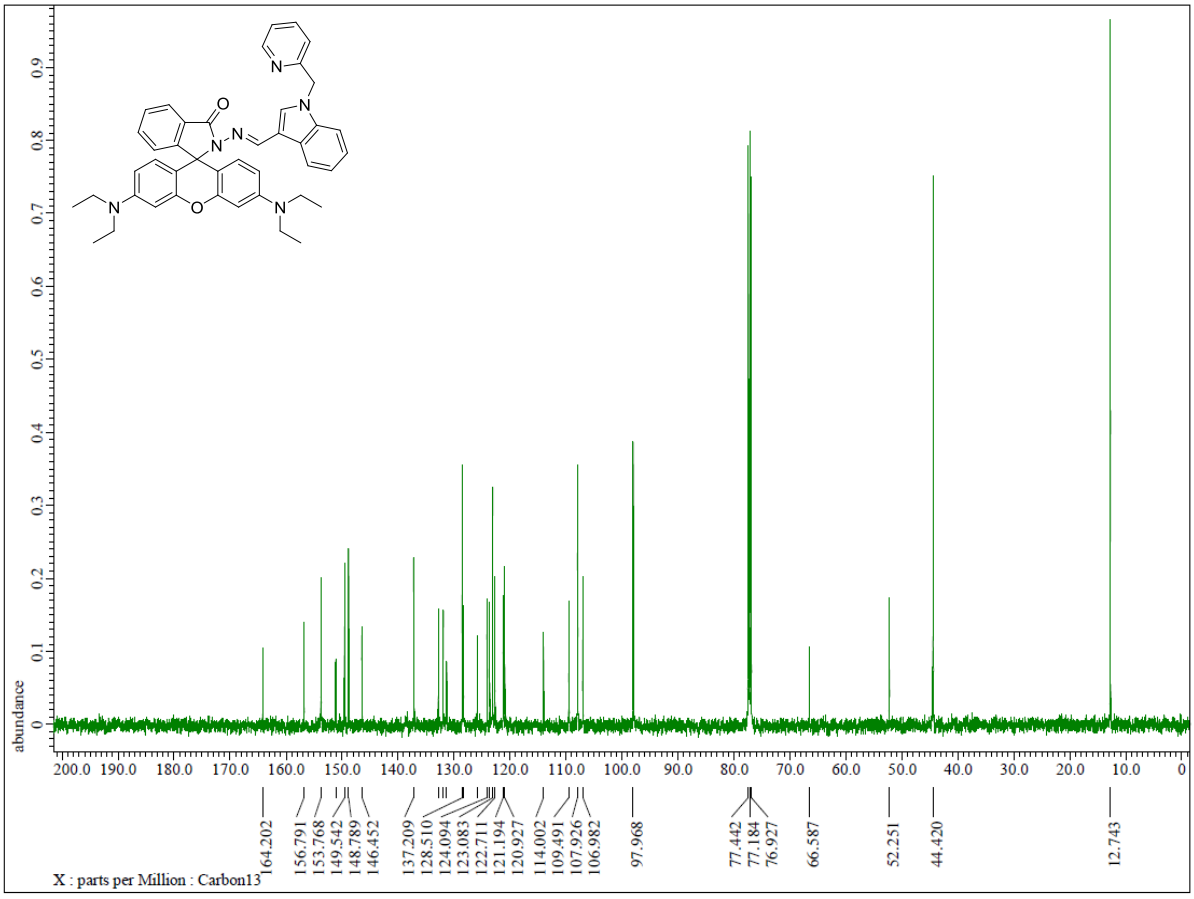

Fig. S2. ^{13}C NMR spectrum of **1** in $CDCl_3$

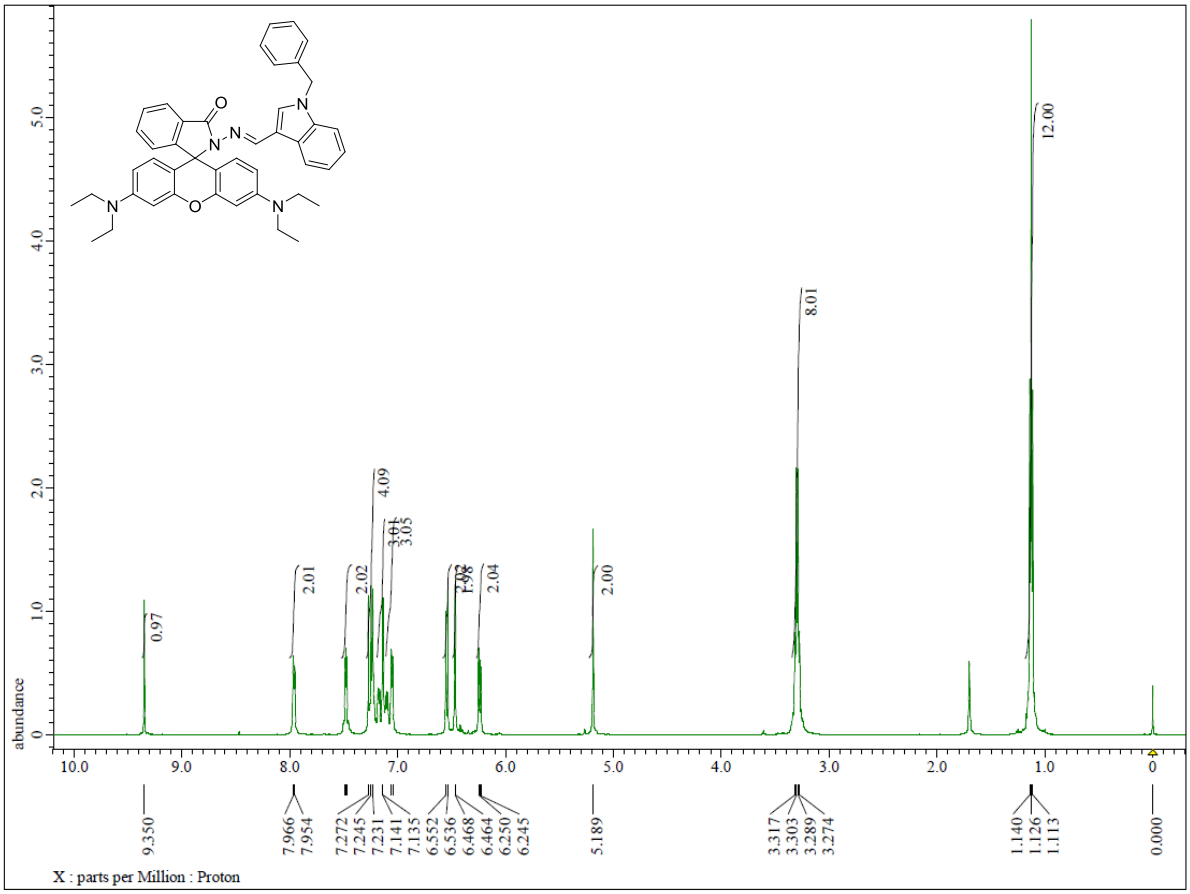

Fig. S3. ^{1}H NMR spectrum of **2** in $CDCl_3$

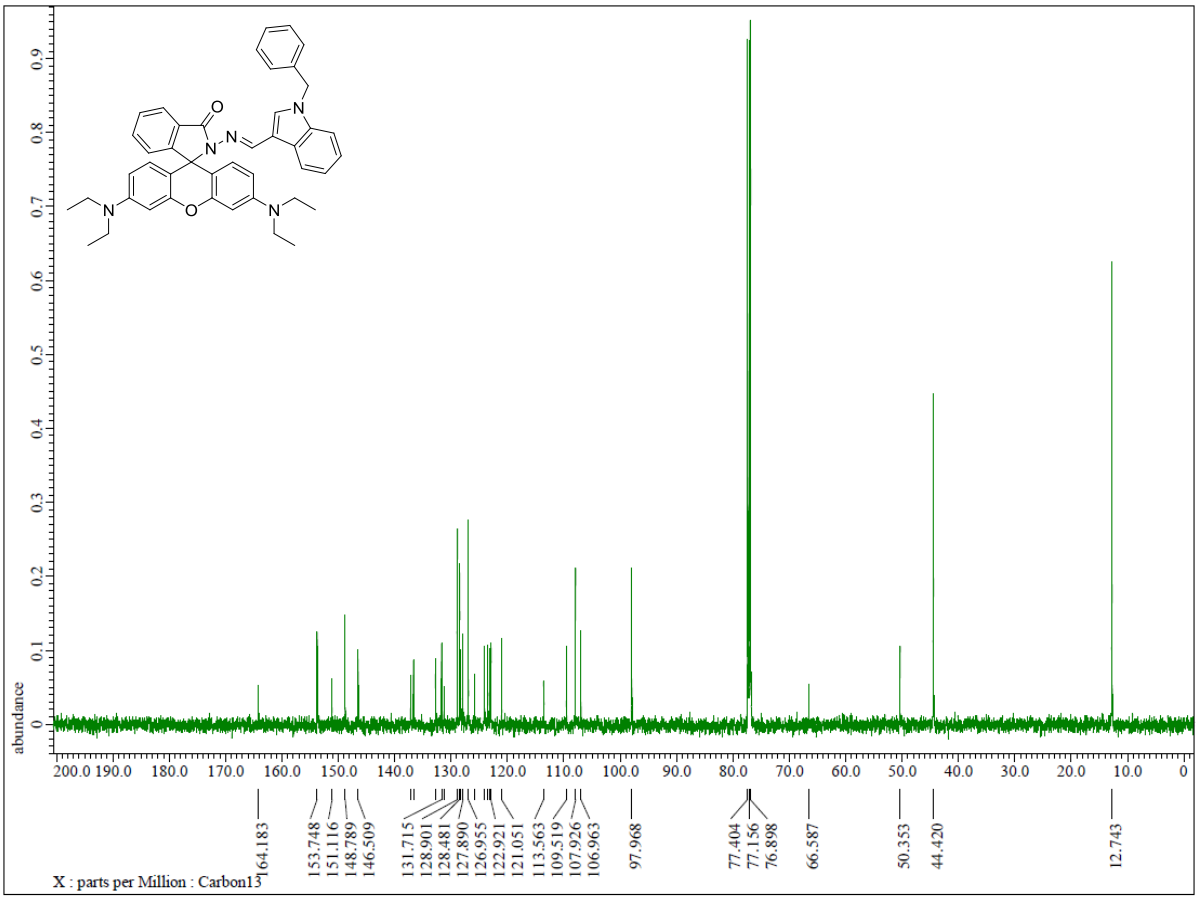

Fig. S4. ^{13}C NMR spectrum of **2** in $CDCl_3$

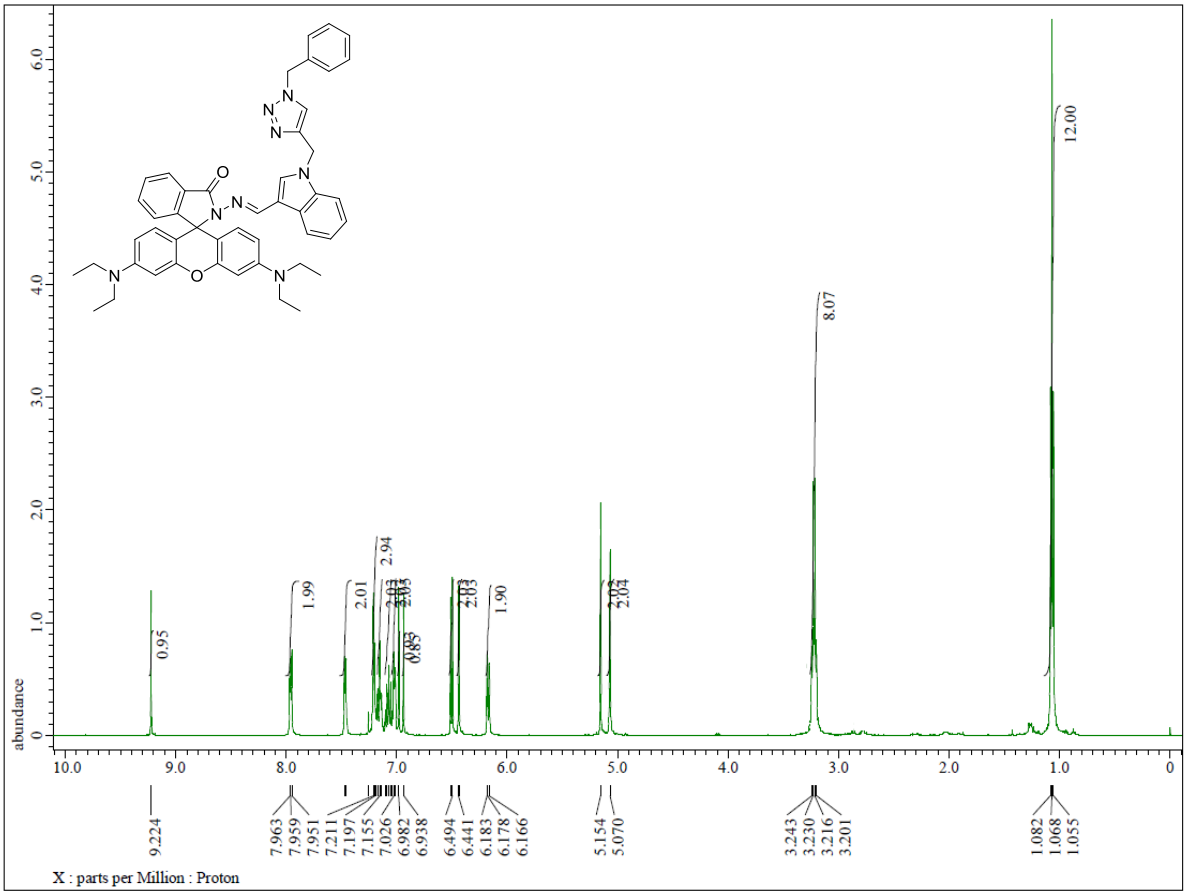

Fig. S5. ^{1}H NMR spectrum of **3** in $CDCl_3$

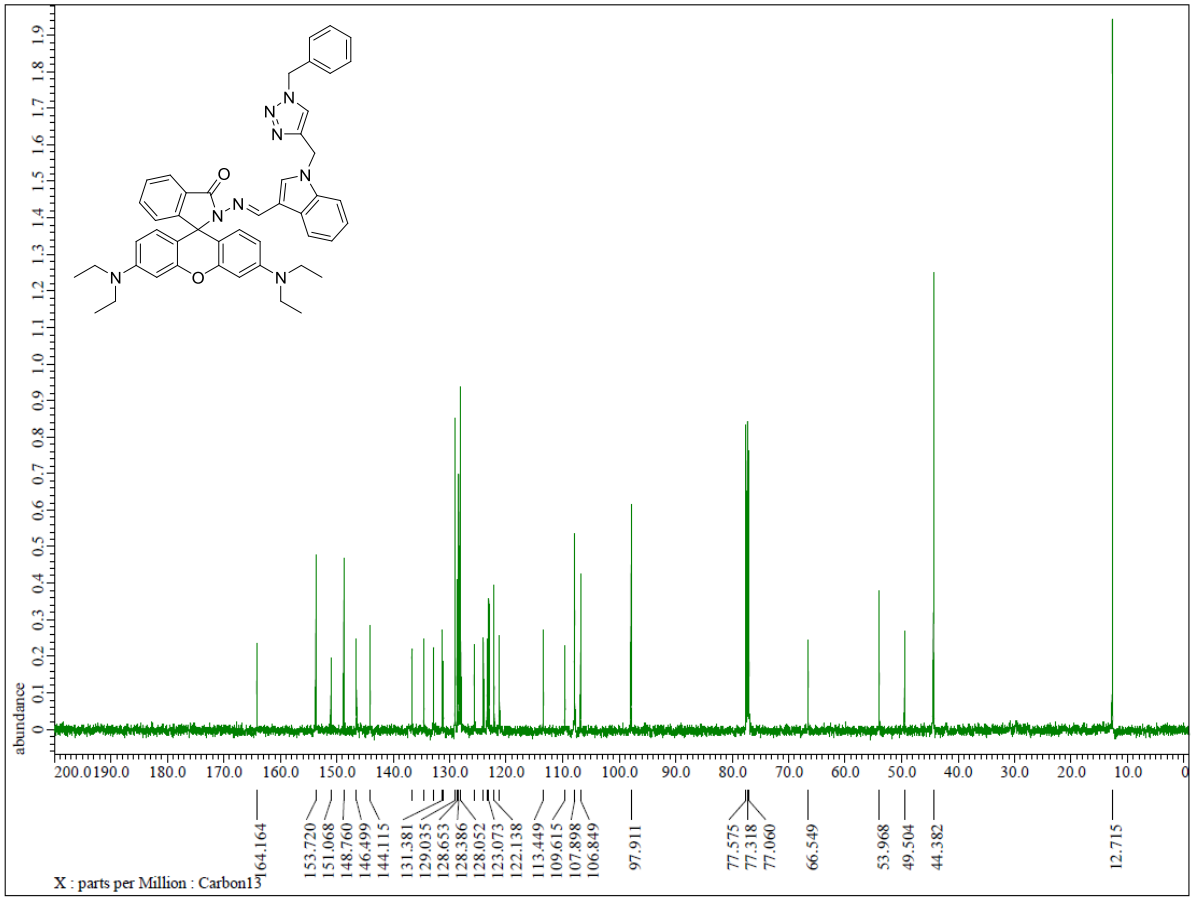

Fig. S6. ^{13}C NMR spectrum of **3** in $CDCl_3$

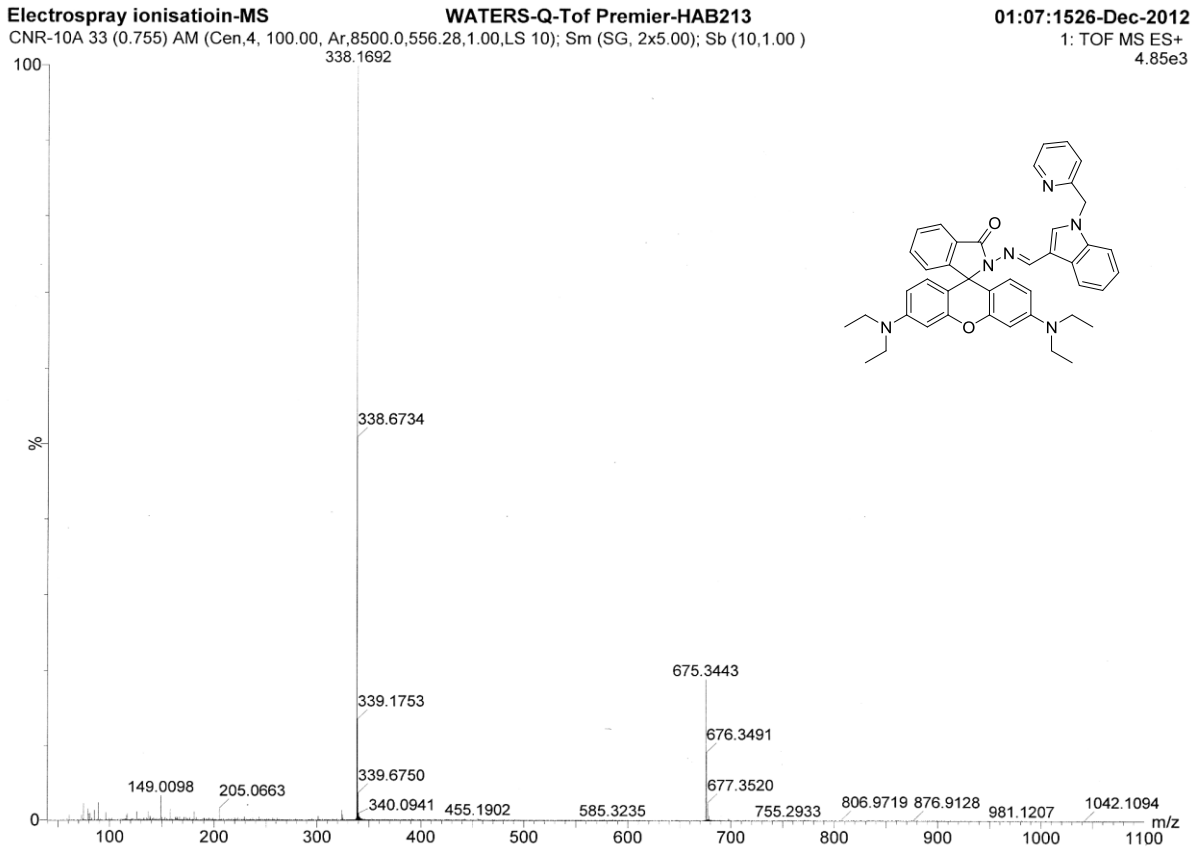

Fig. S7. ESI Mass spectrum of **1**

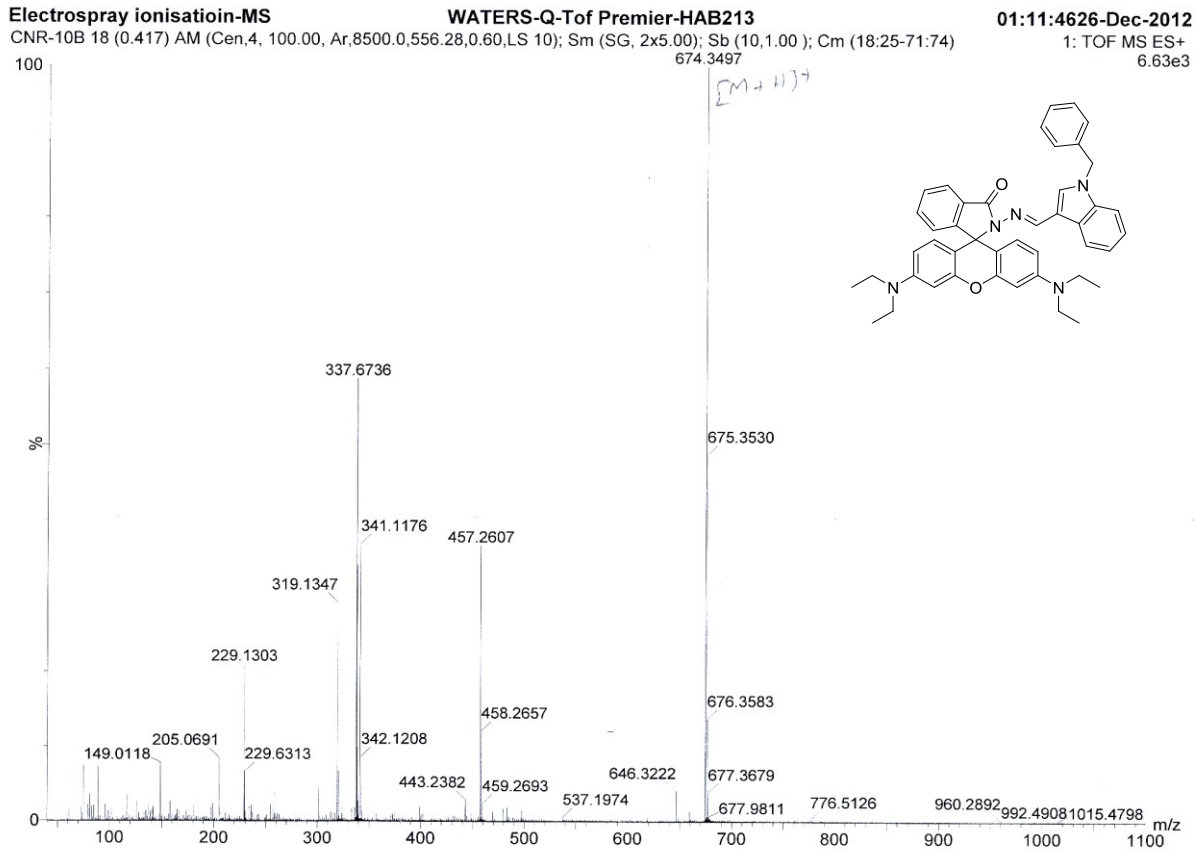

Fig. S8. ESI Mass spectrum of **2**

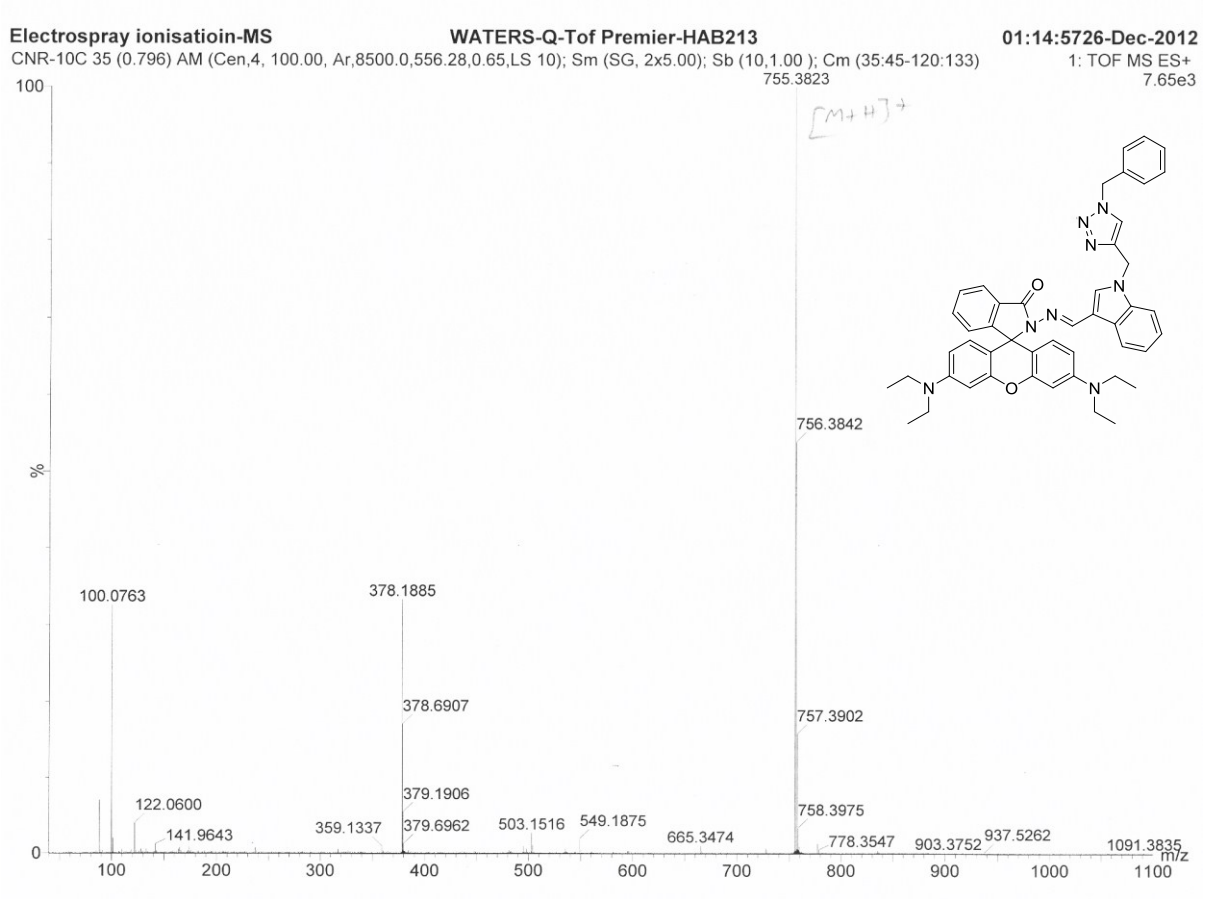

Fig. S9. ESI Mass spectrum of **3**

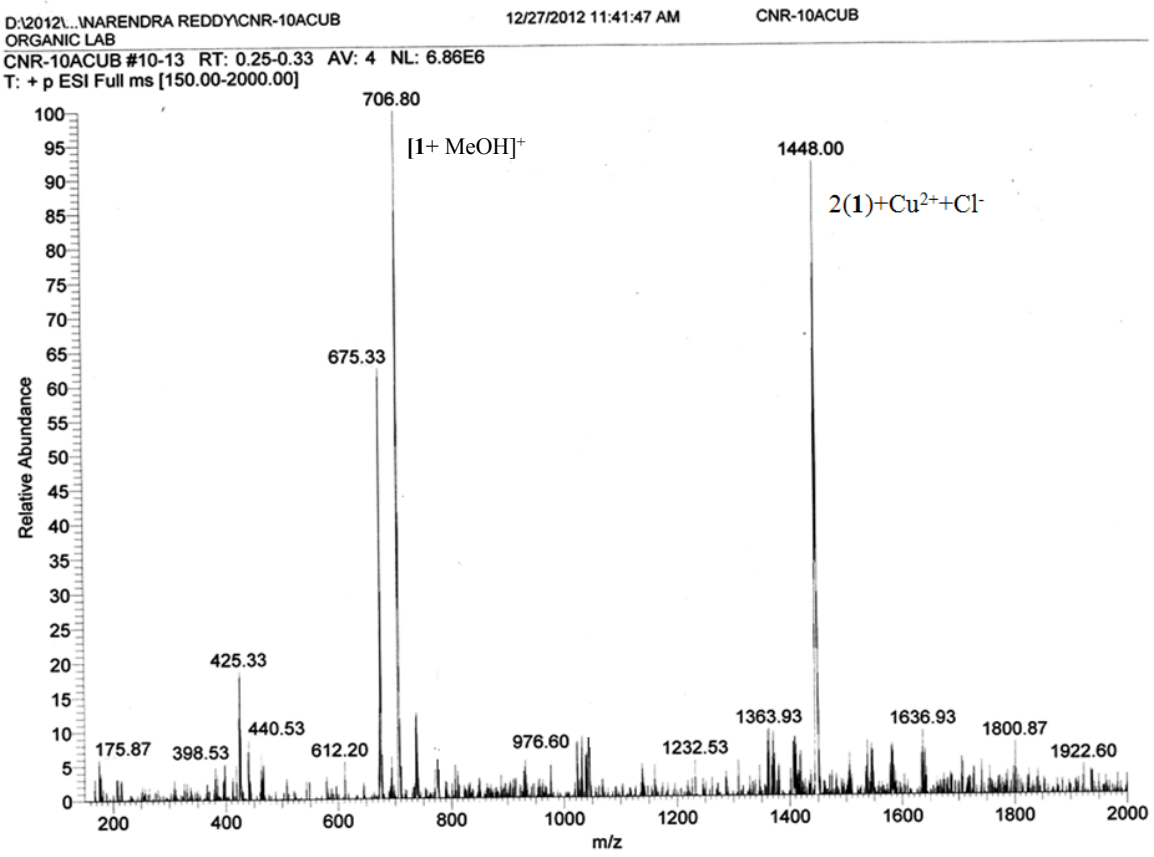

Fig. S10. ESI Mass spectrum of **1-Cu**$^{2+}$ complex

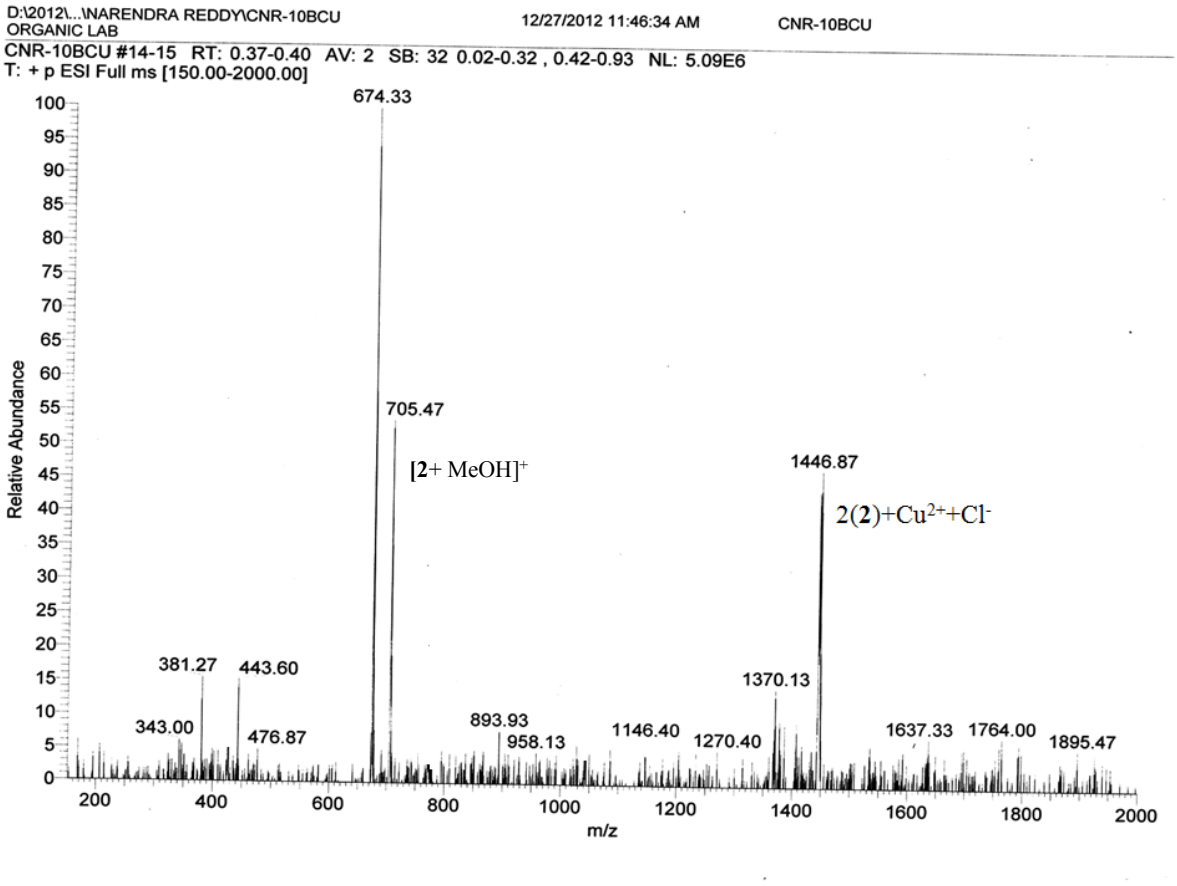

Fig. S11. ESI Mass spectrum of **2-Cu**$^{2+}$ complex

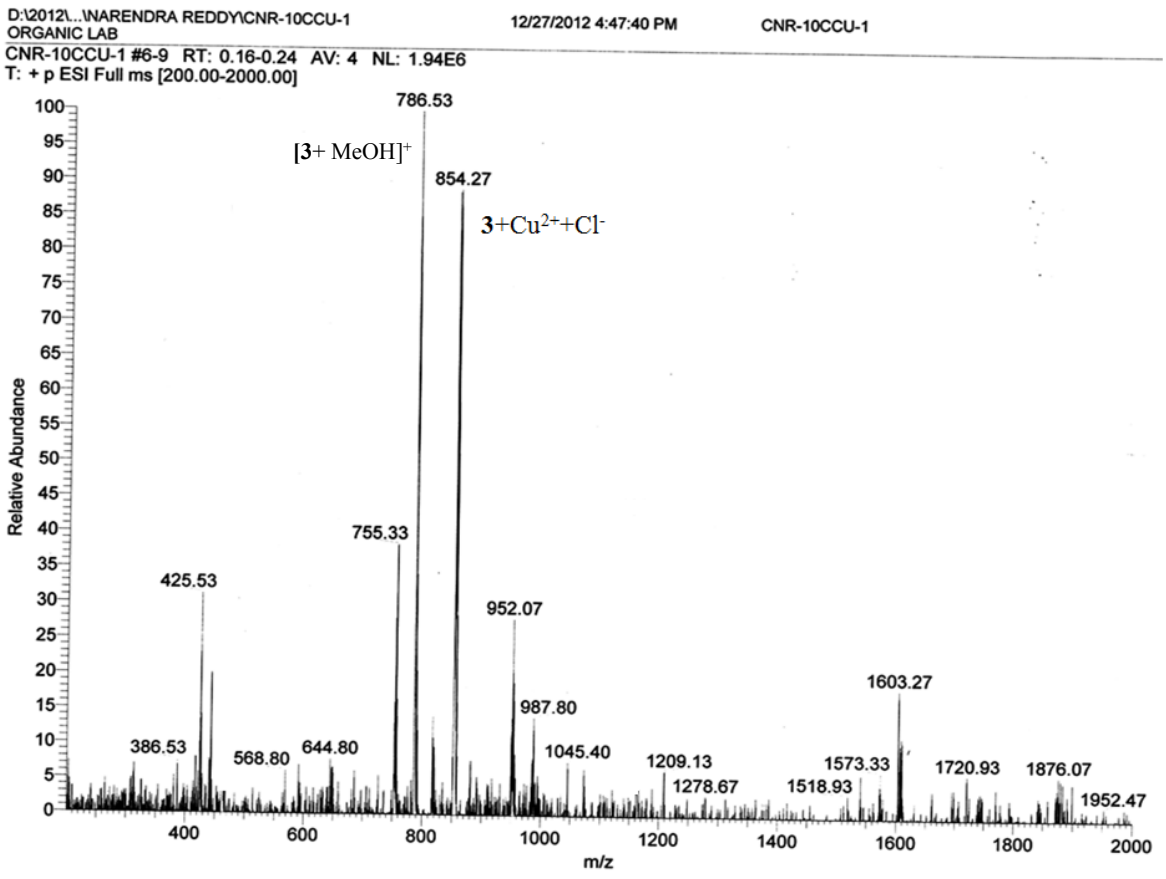

Fig. S12. ESI Mass spectrum of **3-Cu**$^{2+}$ complex

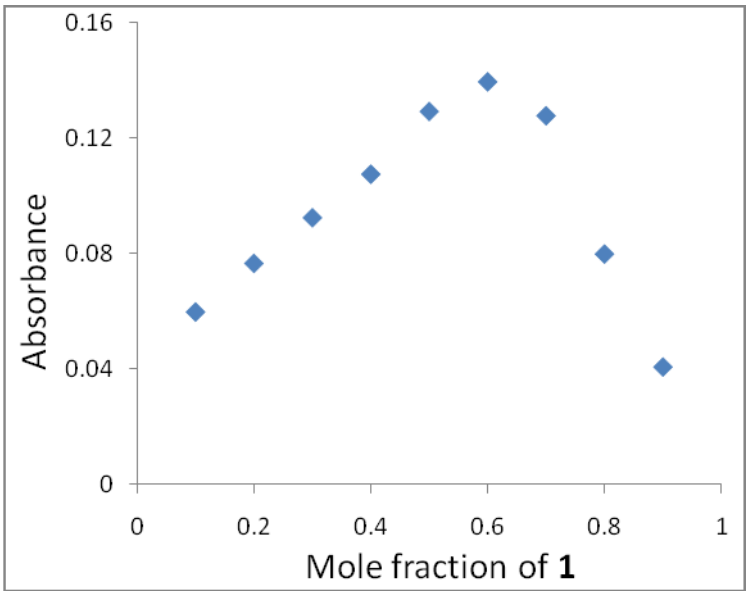

(a)

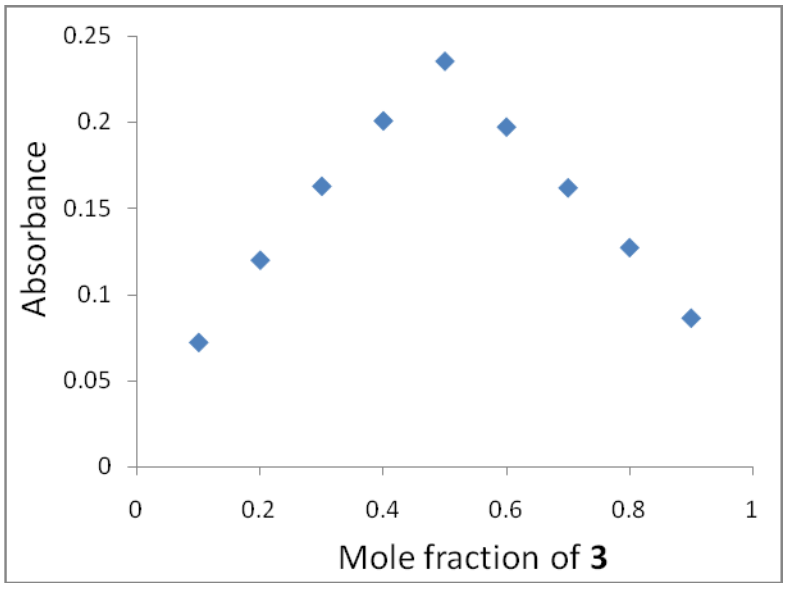

(b)

Fig. S13. The Job plot data of **1**-Cu^{2+} (**a**) and **3**-Cu^{2+} (**b**) complexes

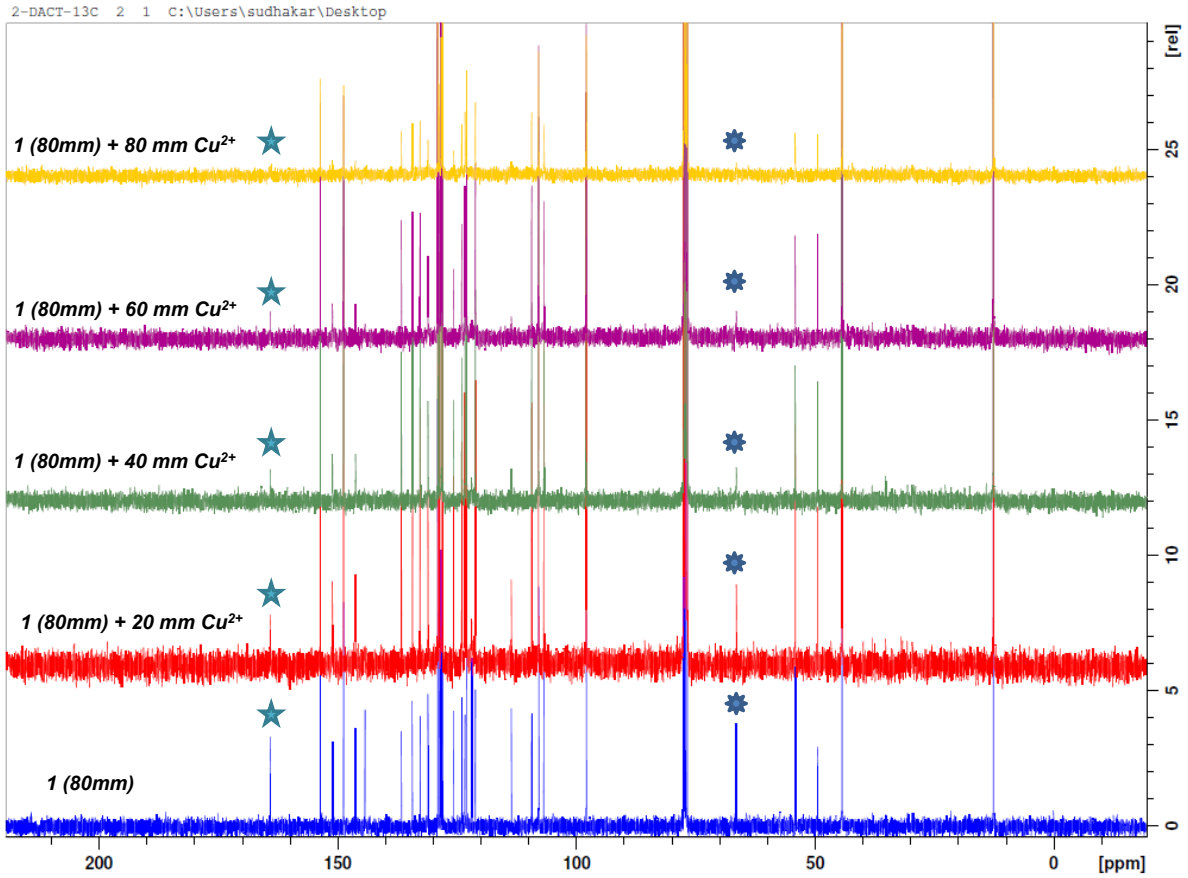

Fig. S14. ^{13}C NMR spectra of **3** in $CDCl_3$ with and without Cu^{2+} ions: The decrease in the intensity of the peaks at 164.23 and 66.57 ppm ascribed to the carbonyl and spiro carbon atoms, respectively, upon addition of indicated concentrations of Cu^{2+} suggest that these atoms are in close proximity to Cu^{2+} ion in the newly formed complex. Due to the paramagnetic nature of copper, a general reduction in the intensity of all ^{13}C signals is also observed at high concentrations of Cu^{2+} ions.[2]

.

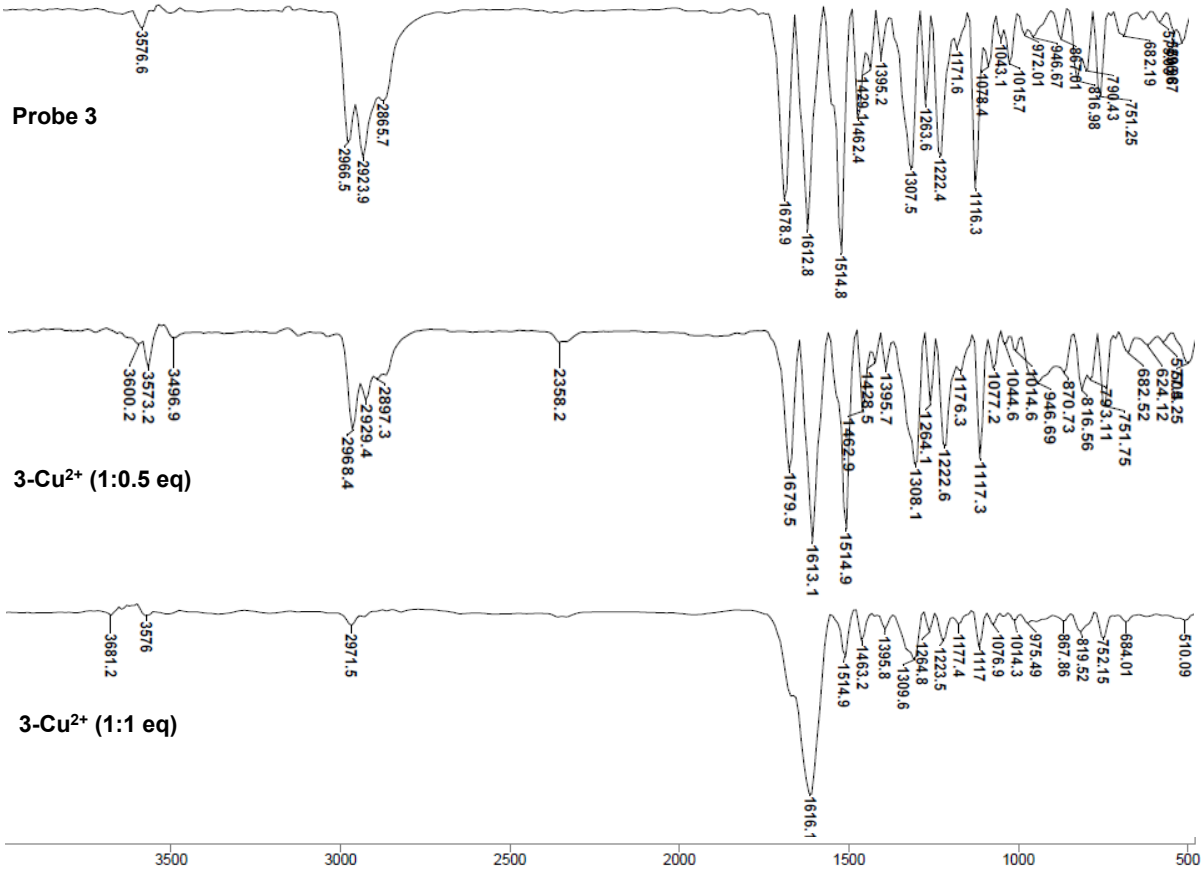

Fig. S15. The FT-IR spectra of **3** in the absence and presence of different concentrations of Cu^{2+}: The reduction in the 'C=O' peak intensity of **3** upon addition of Cu^{2+}, and the absence of any new band corresponding to the acid 'C=O' stretching indicated that the added Cu^{2+} was involved in the complex formation and did not lead to any catalytic action.[3]

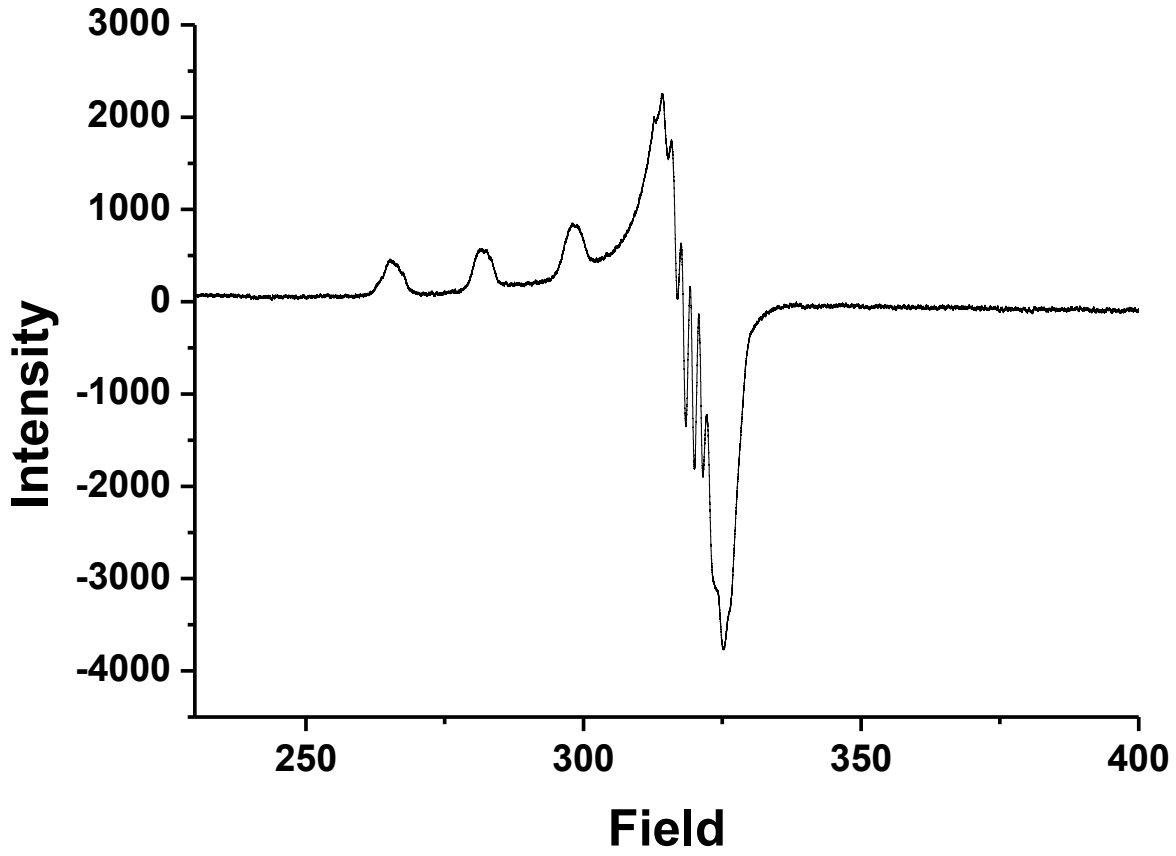

Fig. S16. ESR spectrum of **3-Cu**$^{2+}$ complex: The **3-Cu**$^{2+}$ complex formation was further confirmed using ESR spectroscopic technique. The calculated $g_{\|}$ (2.2548) and $g_{\perp}$ (2.0413) values indicated the tetragonal structure of the complex ($g_{\|} > g_{\perp}$). Similarly, the averaged $A_{\|}$ value (164.577) also supported the tetragonal geometry of the **3-Cu**$^{2+}$ complex. The observed super hyperfine splitting pattern (14.067, 16.014, 17.528, 15.798 and 14.066 guass) clearly established the involvement of 'N' donor atoms in the coordination.[4]

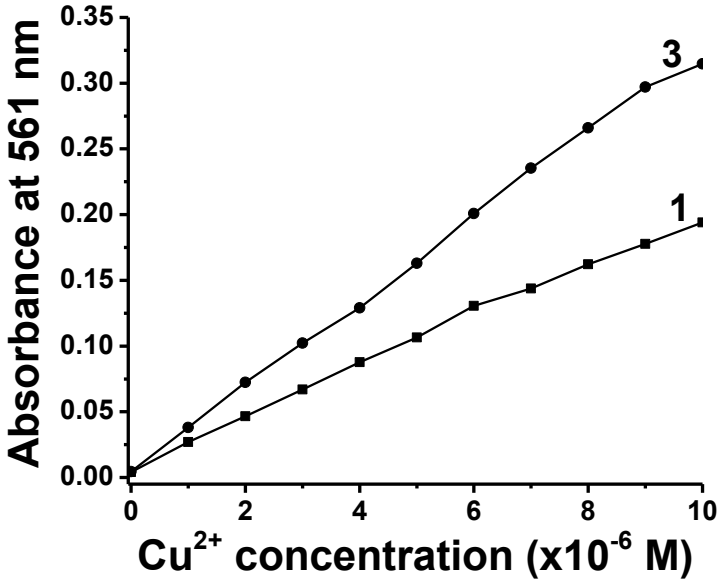

Fig. S17. Variation in the absorption intensity of **1** and **3** upon addition of Cu^{2+}

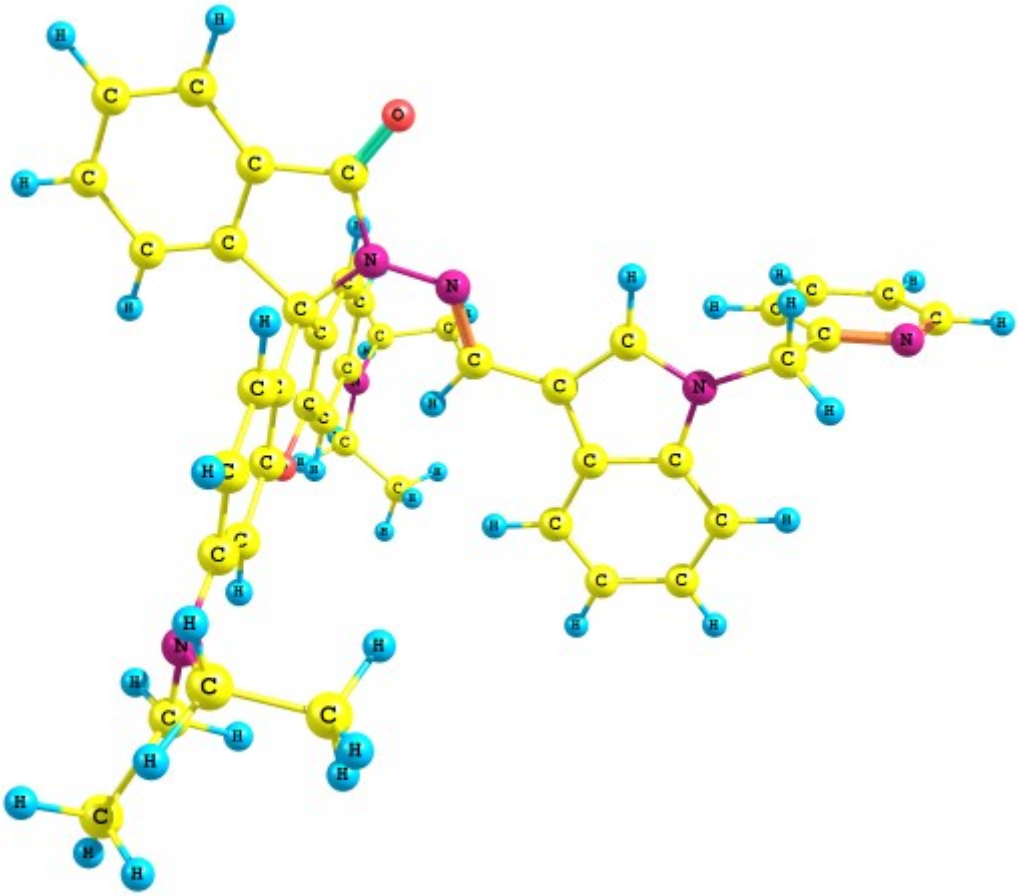

Fig. S18. Gaussian 03; b3lyp/6-31(d) optimized conformation of **1**

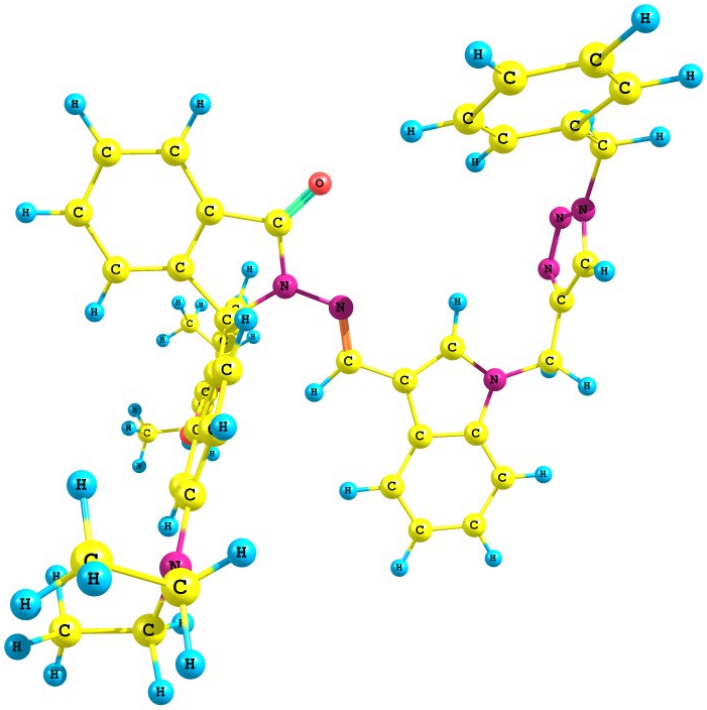

Fig. S19. Gaussian 03; b3lyp/6-31(d) optimized conformation of **3**

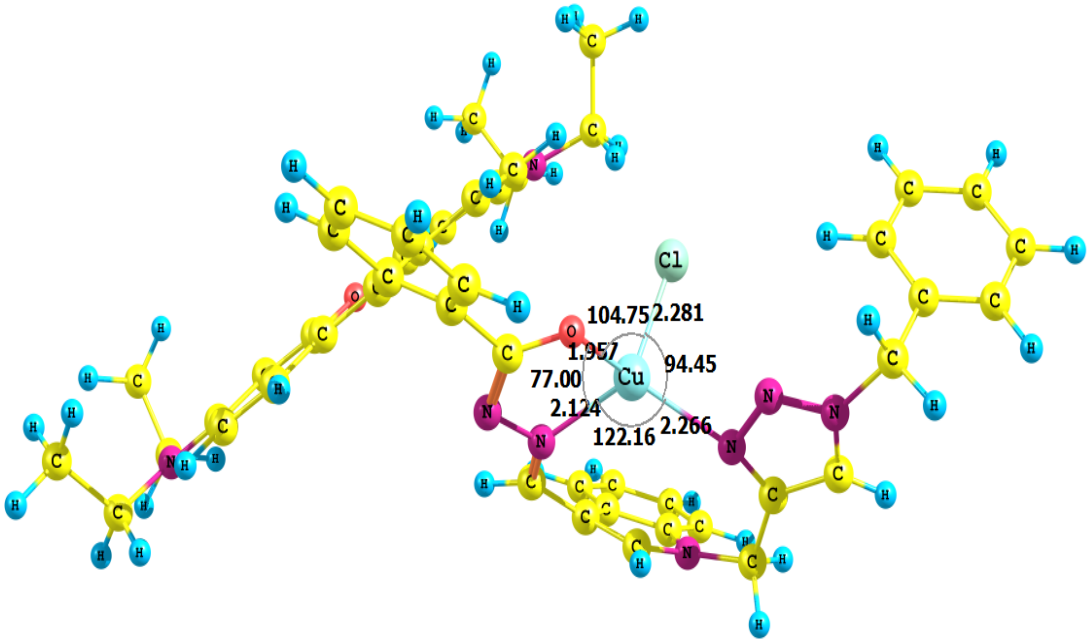

Fig. S20. Gaussian 03; b3lyp/LANL2DZ optimized geometry of **3-Cu**$^{2+}$ complex

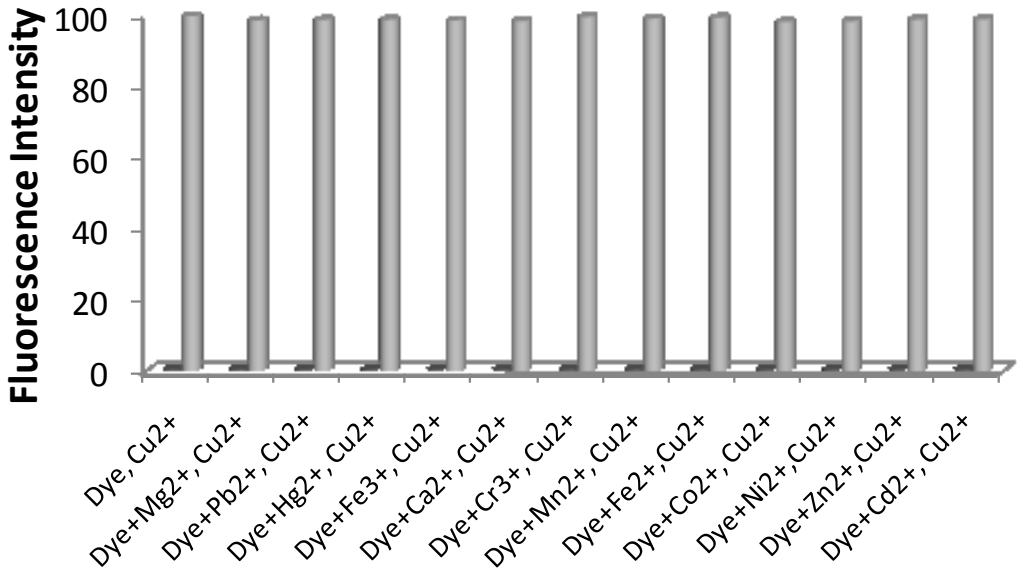

Fig. S21. Metal-ion selectivity of **3** in 1:1 v/v 0.01M Tris HCl-CH_3CN, pH 7.4. The dark bars represent the fluorescence emission at ~580 nm of a solution of **3** (10 μM) and 5 equiv of other metal ions. The light bars show the the fluorescence emission at ~580 nm after the addition of 1 equiv of Cu^{2+} to the solution containing **3** (10 μM) and different metal ions (50 μM).

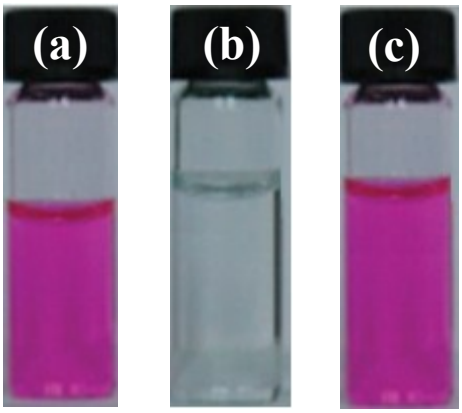

Fig. S22.The reversibility of **3-Cu^{2+}** complex. (**a**) solution of **3** (10 μM) and Cu^{2+} (10 μM) and (**b**) 20 μM of EDTA was added to **a** (**c**) 50 μM of Cu^{2+} was added to **b**

The pink colour of the **3** and Cu^{2+} (10 μM each) solution (**a**) was turned to colourless (**b**) upon addition of EDTA (20 μM) (EDTA was added after 6h from the time of the addition of Cu^{2+} to **3**) confirmed that the Cu^{2+} added to probe **3** was formed complex with **3** and not led any catalytic action. The addition of excess concentation of Cu^{2+} (50 μM) to the above solution [**3** (10 μM), Cu^{2+} (10 μM) and EDTA (20 μM)] resulted in the formation of pink colour (**c**) confirmed the reversibility of **3-Cu^{2+}** complex.

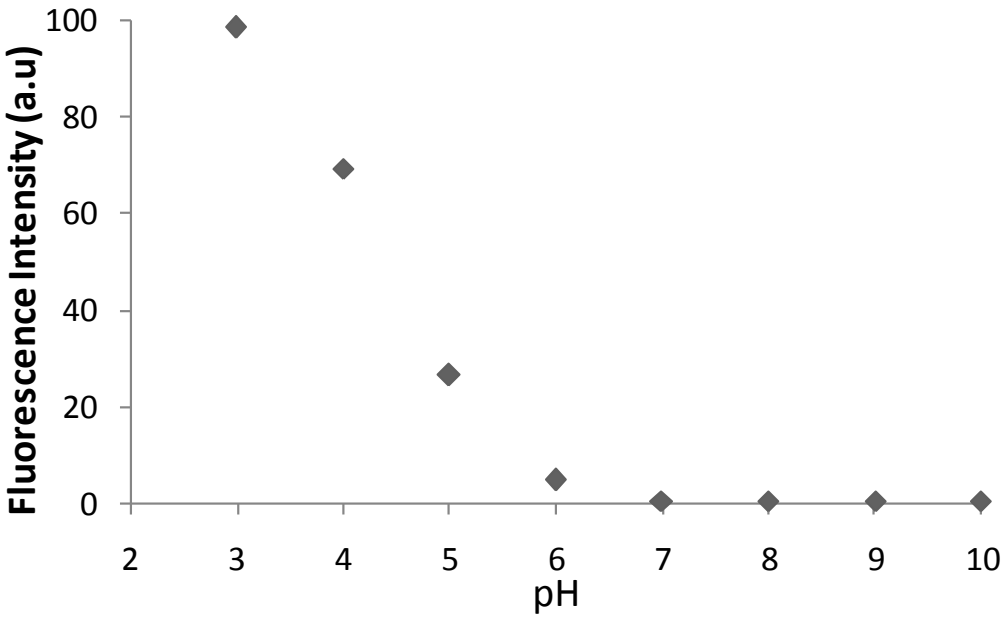

Fig. S23. pH dependant variation in fluorescence intensity of **3** (10 μM) at 580 nm.

Cell viability assay

The cell viability assay of sensor **3** on NIH3T3 cells was determined by MTT (3-(4, 5-Dimethylthiazol-2-yl)-2, 5- diphenyltetrazolium bromide) assay (*J Immunol Methods*, 1983, **65**, 55.). The NIH3T3 cells were trypsinised and seeded in 48-well flat-bottom culture plates at a density of 4 x 10^3 cells per well in 250 µL DMEM supplemented with 10% FBS, 100 IU/mL penicillin, 100 µg/mL streptomycin, 30 µg/mL gentamicin. The cells were allowed for 24 hours to adhere and grow at 37 ºC in CO_2 incubator. Then the medium was replaced with 250 µL fresh medium containing various concentrations of sensor **3** (0 to 25 µM) and incubated for 12 hours in a humidified chamber with 5% CO_2 after which the medium was removed. The cells were further incubated for 3 hours with 250 µL of fresh medium containing 1 mg/mL MTT reagent. The medium was then removed to eliminate unreacted MTT reagent. DMSO (100 µL) was added into each well to dissolve the formazan precipitate formed and was measured spectrophotometrically using a microplate reader at 570 nm. The assay was performed in quadruplet for each concentration. The cytotoxicity of the sensor **3** was expressed in terms of percentage of cell viability relative to the untreated control cells which was taken as 100 percent viable.

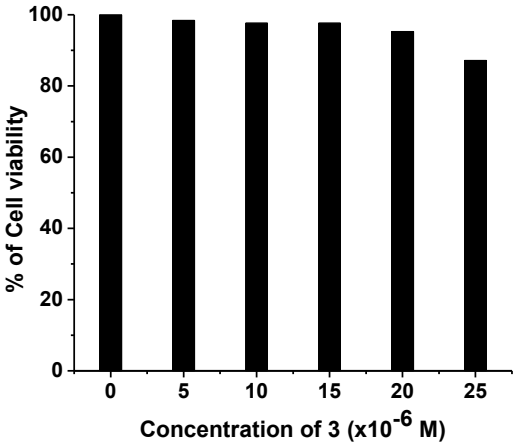

Fig. S24. The cell viability percentage of NIH 3T3 cells after treatment with different concentrations of sensor **3**.

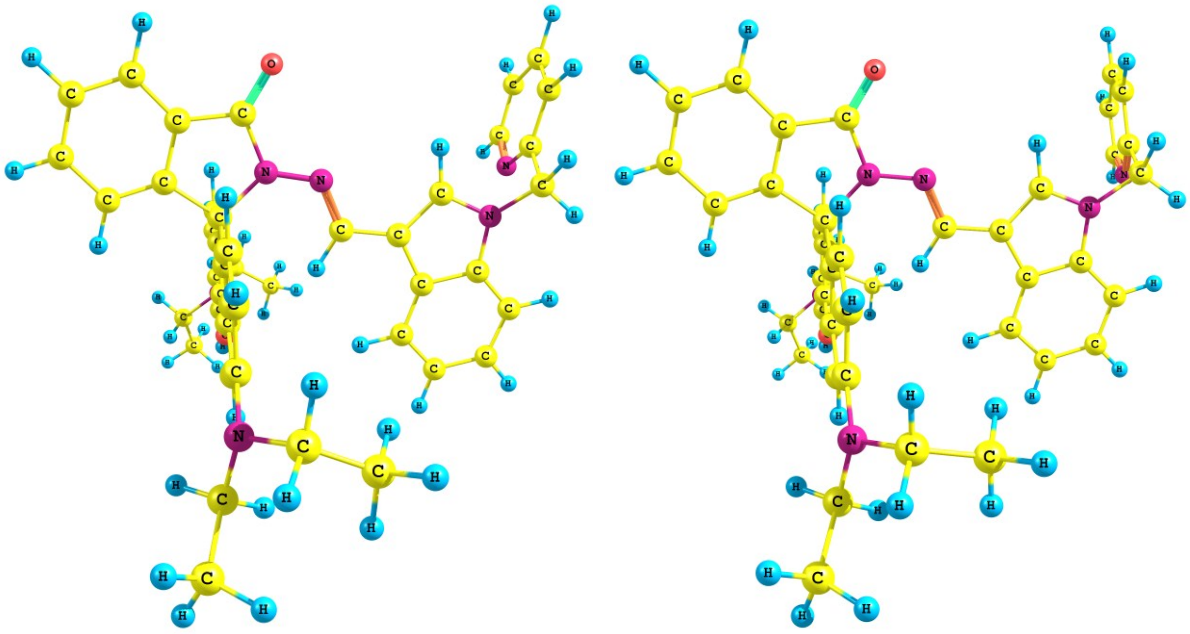

(**a**) E = -2142.78327076 A.U. (**b**) E = -2142.80958119 A.U.

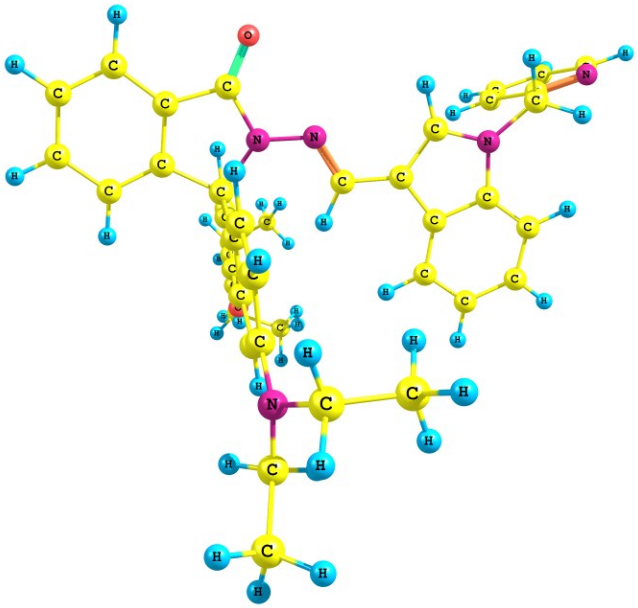

(**c**) E = -2142.82026299 A.U.

Fig. S25. Gaussian 03; b3lyp/6-31(d) level optimized structures and energies of different conformers of **1:** The conformer of **1** with pyridine 'N' pointing 'in' (**a**) was less stable compared to the one in which the 'N' is pointing 'out' (**c**) by an energy of 0.03699 A.U (97 kJ/mol).

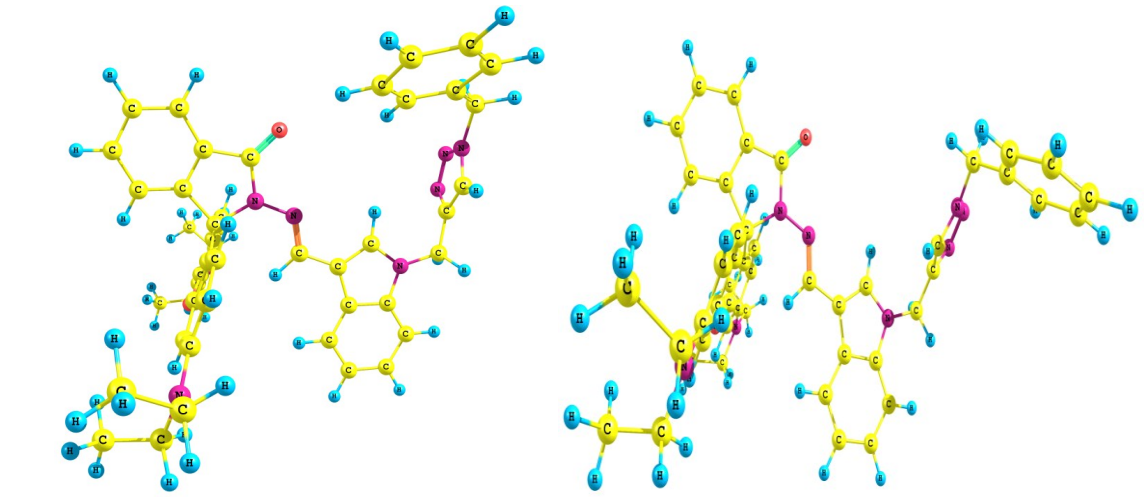

(**a**) E = -2407.12917109 A.U. (**b**) E = -2407.12575248 A.U.

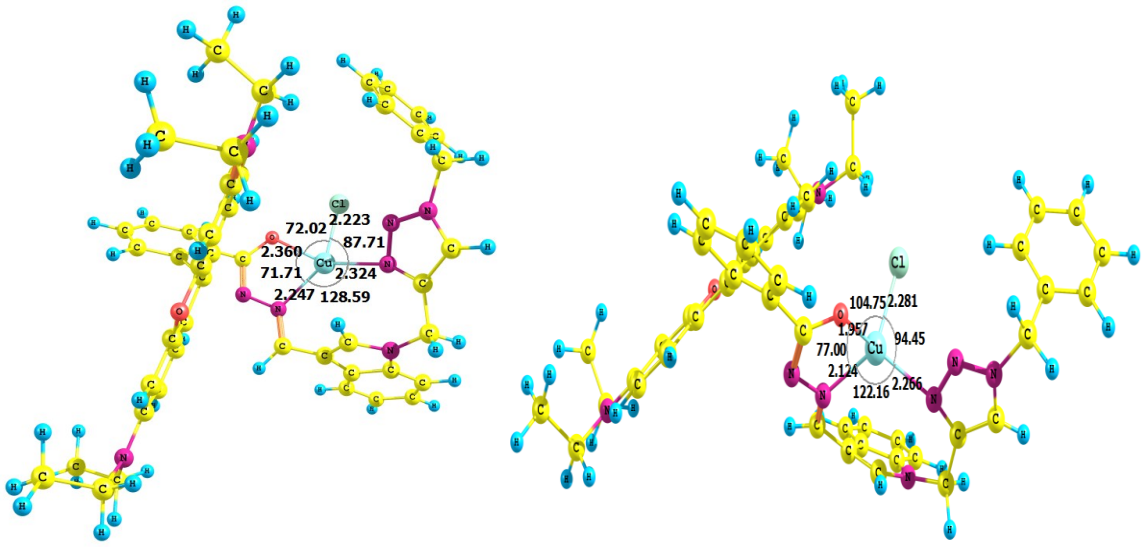

(**c**) E = -3063.15699828 A.U. (**d**) E = -3063.31284766 A.U.

Fig. S26. Gaussian 03; b3lyp/LANL2DZ optimized structures and energies of different conformers of **3** and **3-Cu** complex: Two conformers' *viz*. phenyl ring 'in' (**a**) and phenyl ring 'out' (**b**) of **3** differ in energy by only 9 kJ/mol. This small energy difference implies that inter conversion between these two conformers is quiet possible. The energy difference between the two conformers of 3-Cu(II) complex is ~409 kJ/mol. Therefore, the conformational flexibility of the triazole arm might favour the formation 3-Cu(II) complex with "phenyl ring out" conformation.

References

1. J.-A. Gan, Q. L. Song , X. Y. Hou , K. Chen and H. Tian, *J. Photochem. Photobiol. A–Chem.,* 2004, **162**, 399.
2. N. R. Chereddy and S. Thennarasu, *Dyes Pigm*., 2011, **91**, 378.
3. N. R. Chereddy, S. Thennarasu and A. B. Mandal, *Sens. Actuators, B*, 2012, **171–172**, 294.
4. I. Gamba,. I. Mutikainen,. E. Bouwman,. J. Reedijk and S. Bonnet, *Eur. J. Inorg. Chem*., 2013, 115.